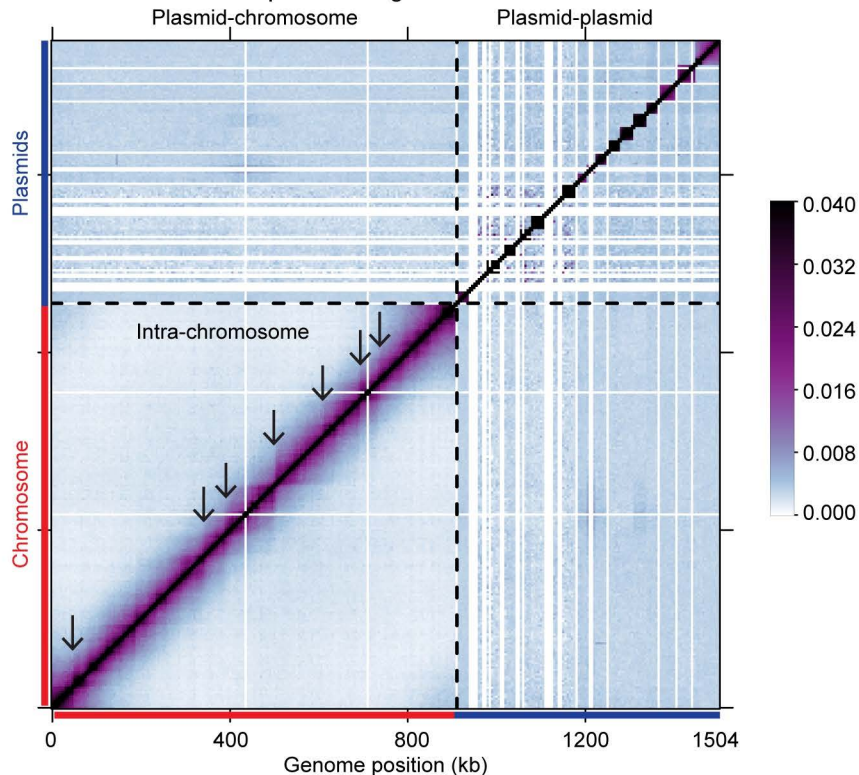
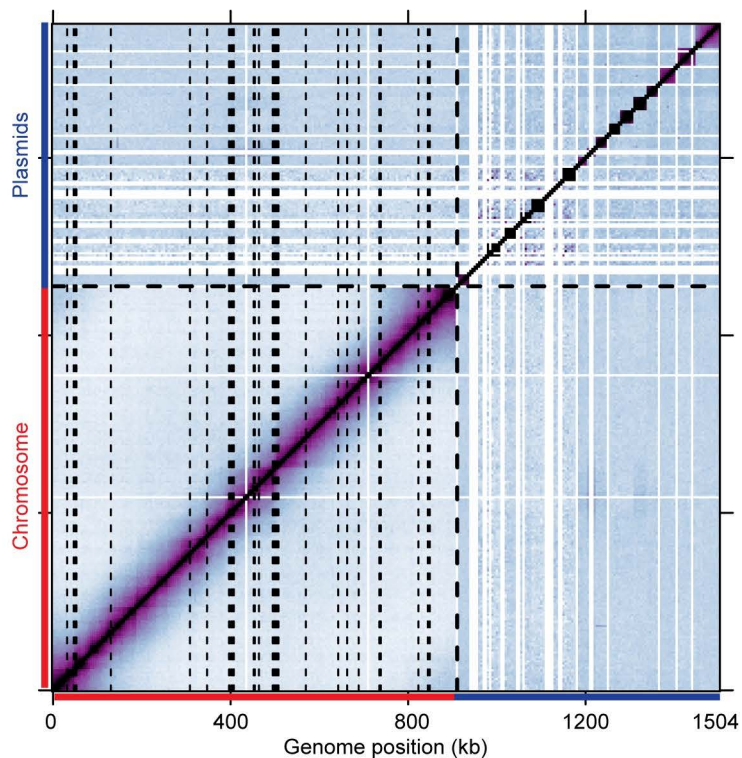


A

Hi-C map of *B. burgdorferi* strain S9

B



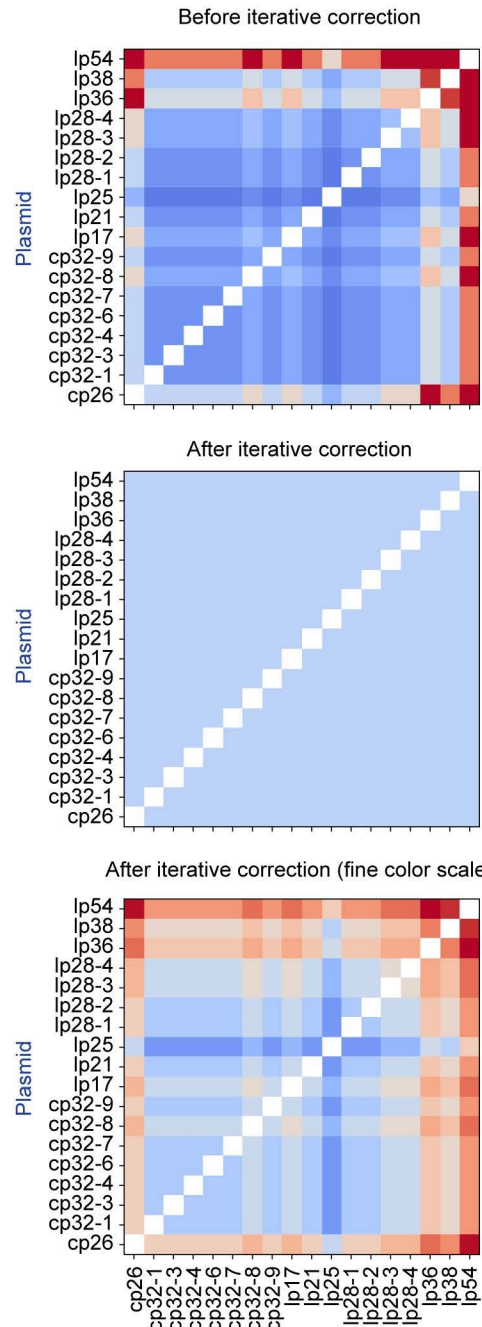
**S1 Fig. Hi-C interaction map of *B. burgdorferi* strain S9 shown in a different color scale.**

**(A)** To better show the intra-chromosomal interactions in **Fig 1B**, the normalized Hi-C interaction map is shown in a different color scale. Black arrows point to a few examples of strong CID boundaries that overlap with highly transcribed genes shown in **(B)**. The color scale depicting Hi-C interaction scores in arbitrary units is shown at the right.

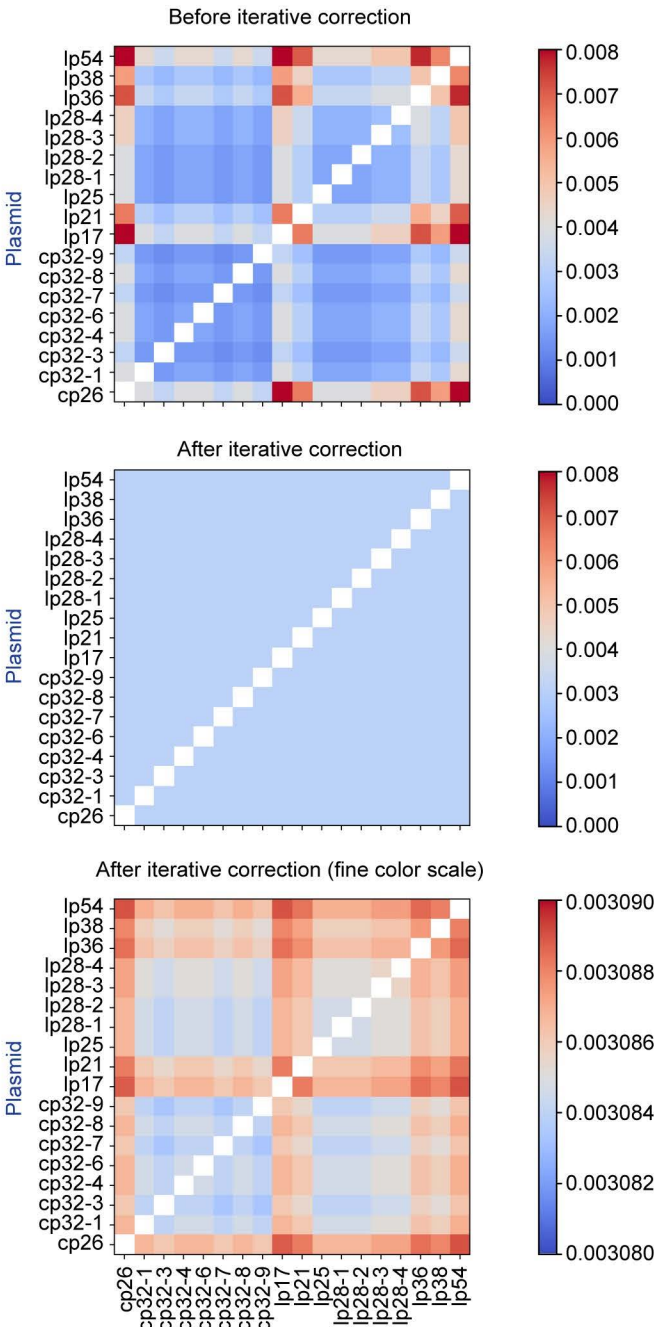
**(B)** The positions of the top 50 highly transcribed chromosomal genes found by RNA-seq [46] are indicated using fine black dotted lines. A recent study [46] published RNA-seq data of the *B. burgdorferi* B31-S9 strain grown in culture. We mapped the data to the *B. burgdorferi* B31 genome, calculated the number of transcripts per kilobase per million reads for each gene, and indicated the top 50 highly transcribed genes on the Hi-C map. Although the growth condition in our study was different from the RNA-seq study [46], strong CIDs boundaries (black arrows in **A**) largely overlap with highly transcribed genes.

**A**

Simulated plasmid-plasmid interactions  
using plasmid copy number and size

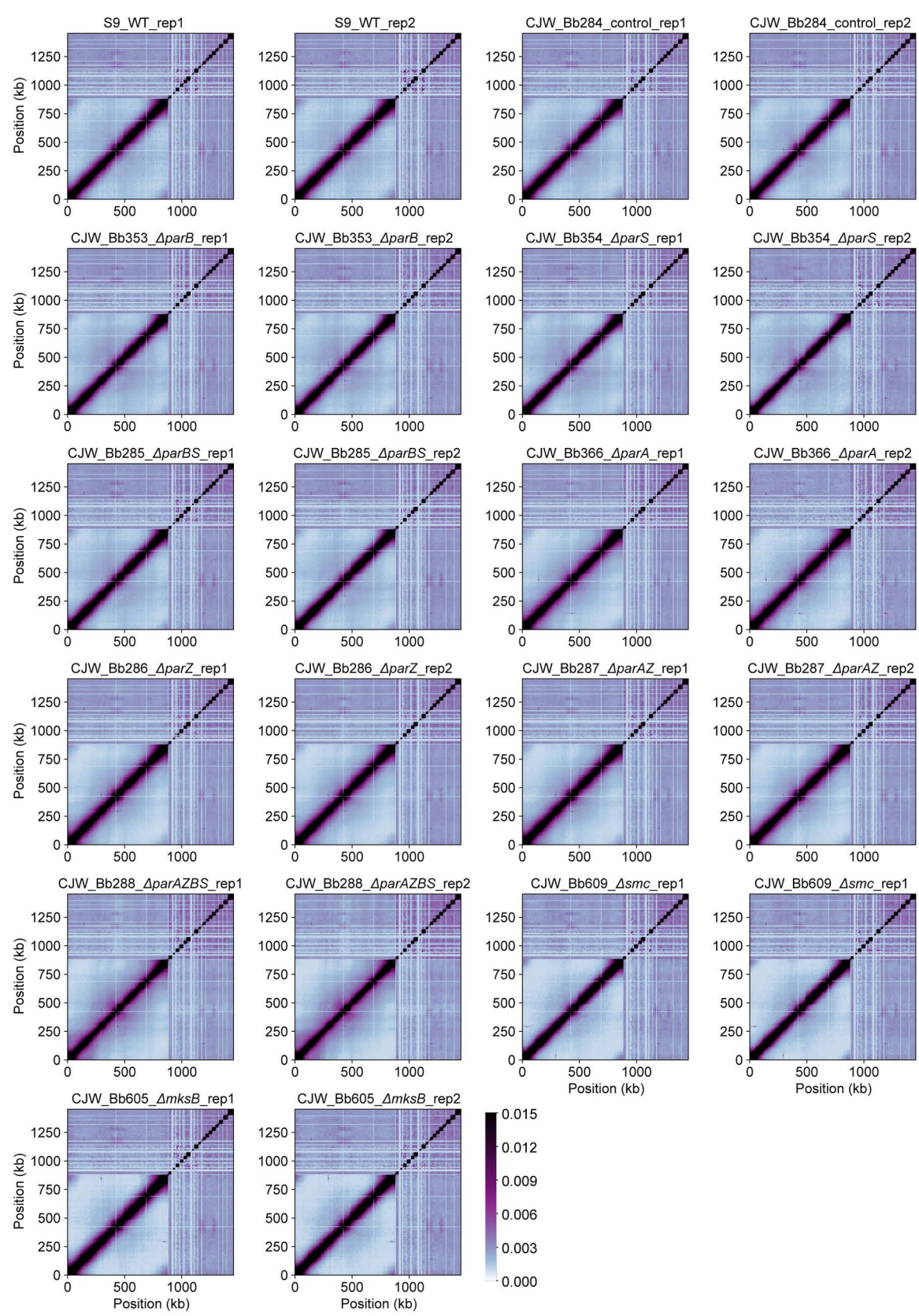
**B**

Simulated plasmid-plasmid interactions  
using plasmid copy number only



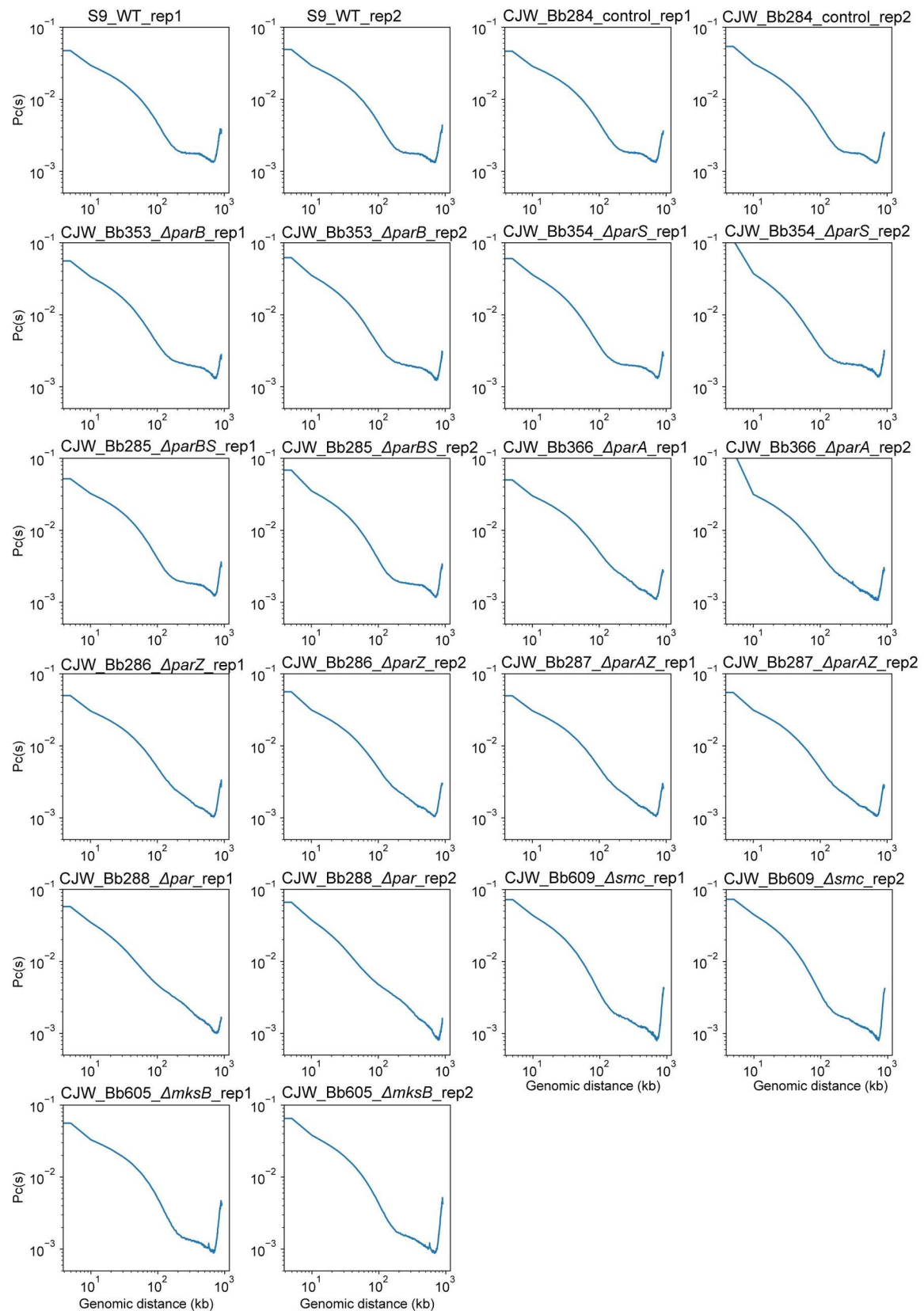
## **S2 Fig. Simulated plasmid-plasmid interaction frequencies.**

The contact probability between plasmids was simulated under the assumptions that plasmids are randomly interacting, independent of one another, and are “well mixed” within the cytoplasm (see Materials and methods). The calculation was performed accounting for plasmid copy numbers and plasmid lengths together (**A**) or only plasmid copy numbers (**B**). Top panels, the raw contact frequency expected between plasmids without normalization. Middle panels, the simulated contact frequency after normalization using iterative correction. Bottom panels, the same as middle panels, but shown with a much finer color scale. The color scales depicting contact frequencies in arbitrary units are shown at the right. We note that there is residual resemblance between bottom and top panels, and in the bottom panel, the row or column sums do not appear to be the same. This is because the iterative correction procedure stops when the row and column sums approach 1 within a pre-defined error tolerance (see Materials and methods), but not exactly at 1.



**S3 Fig. Hi-C samples used in this study.**

The normalized Hi-C interaction maps of all 22 experiments done for this study. The color scale depicting Hi-C interaction scores is shown at the bottom right.

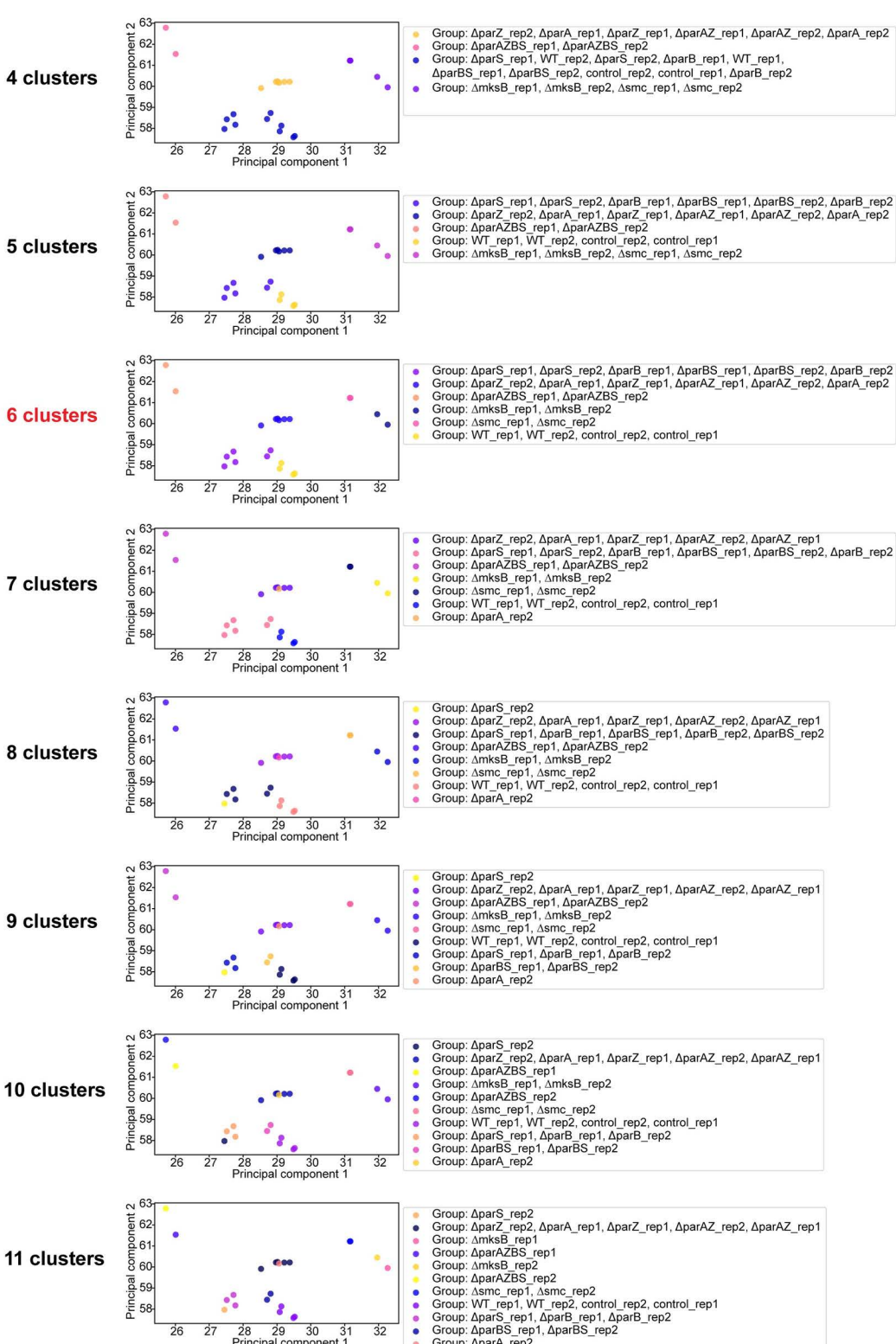


**S4 Fig. Individual  $Pc(s)$  curves of all the samples analyzed in this study.**

$Pc(s)$  curves of all 22 Hi-C experiments done in this study. The x-axis indicates genomic distance while the y-axis shows averaged contact frequency. Only intra-chromosomal interactions were used to calculate the  $Pc(s)$  curves.

# PCA with groups from K-means clustering on log(Pc(s)) curves

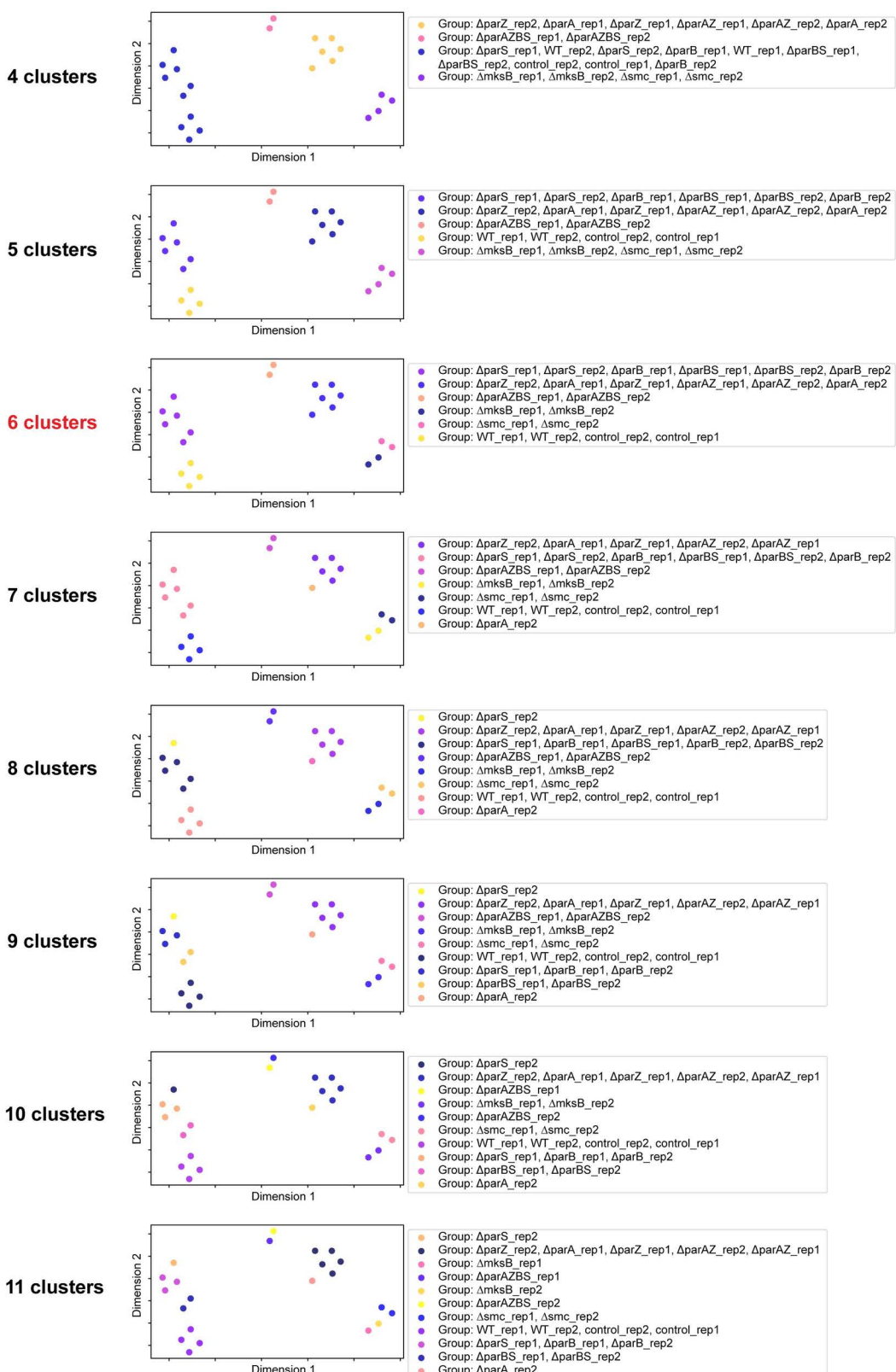
Components 1 and 2 explain 48% and 37% of the variance, respectively



**S5 Fig. Principal Component Analysis (PCA) with groups from k-means clustering results.**

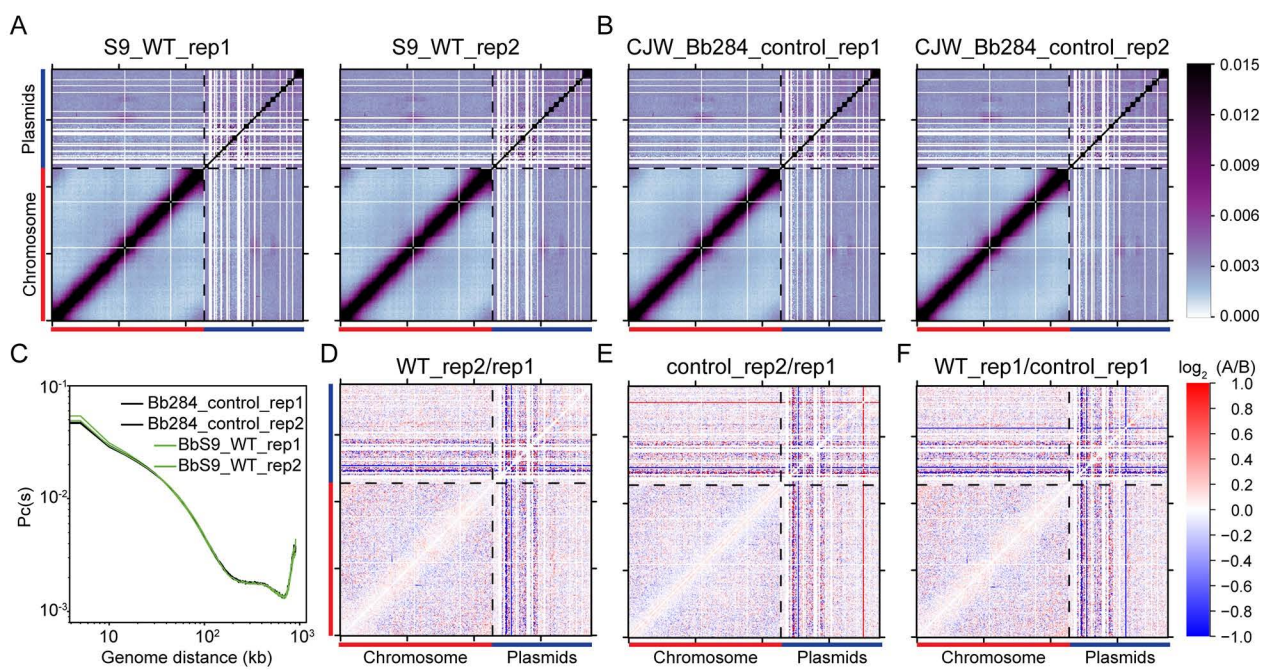
To better visualize the results of the k-means clustering generated by the Silhouette method, we performed Principal Component Analysis (PCA) and labeled the clustering results (see Materials and methods). The plots with up to six clusters gave nicely visually segregated groups. Beyond six, the two-dimensional projections from PCA showed poor segregation of the data points, and biological replicates were separated to different groups.

# T-distributed stochastic neighbor embedding with groups from K-means clustering on log(Pc(s)) curves



**S6 Fig. T-distributed stochastic neighbor embedding (t-SNE) with groups from k-means clustering results.**

To better visualize the results of the k-means clustering generated by the Silhouette method, we performed t-distributed stochastic neighbor embedding (t-SNE) and labeled the clustering results (see Materials and methods). Similar to PCA, the plots with up to six clusters gave nicely visually segregated groups. Beyond six, the two-dimensional projections from t-SNE showed poor segregation of the data points, and biological replicates were separated to different groups.

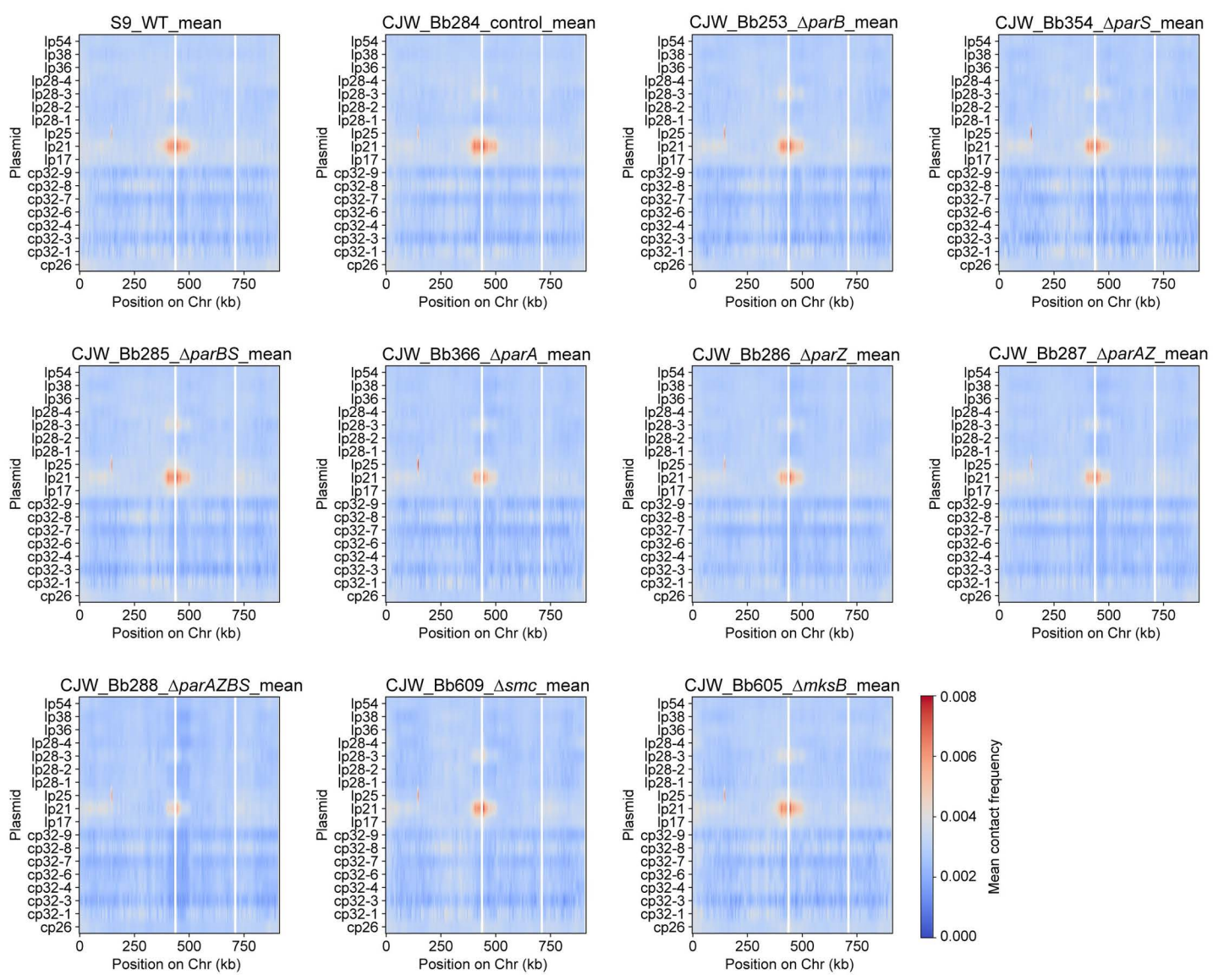


**S7 Fig. Comparison of WT and control strains.**

**(A-B)** Normalized Hi-C interaction maps of *B. burgdorferi* strains S9 (WT) and the control strain CJW\_Bb284. Two biological replicates of each strain (rep1 and rep2) are shown. The color scale depicting Hi-C interaction scores in arbitrary units is shown at the right.

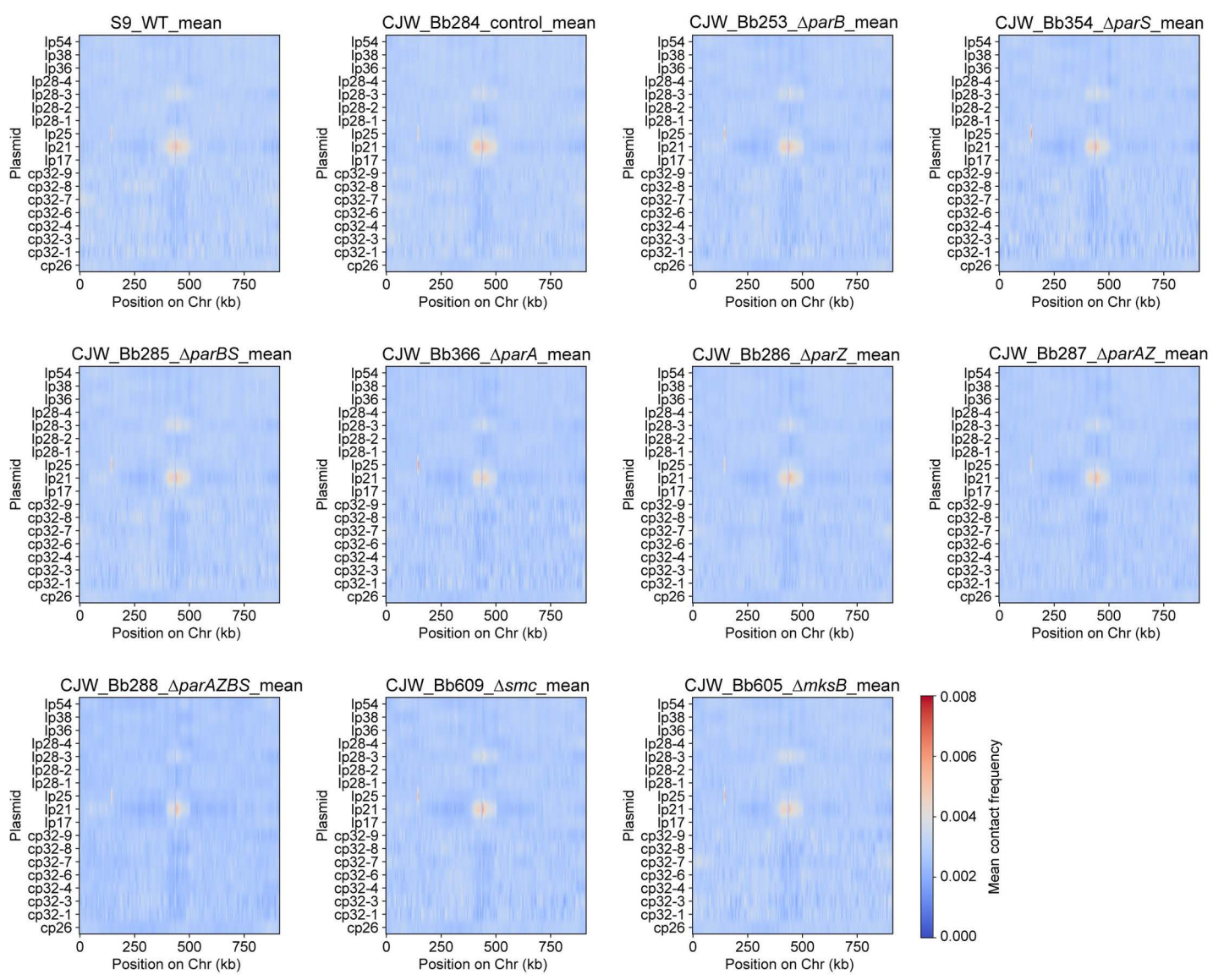
**(C)**  $Pc(s)$  curves of the four samples.  $Pc(s)$  curves show the averaged contact frequency between all pairs of loci on the chromosome separated by set distance ( $s$ ). The x-axis indicates the genomic distance of separation in kb. The y-axis represents the averaged contact frequency. The curves were computed for data binned at 5 kb. Only intra-chromosomal interactions were used to calculate the  $Pc(s)$  curves.

**(D-F)**  $\log_2$  ratio plots comparing different Hi-C matrices.  $\log_2(\text{matrix 1}/\text{matrix 2})$  was calculated and plotted in the heatmaps. The identities matrix 1/matrix 2 are shown at the top of each plot. The color scale is shown at the right of panel (F).



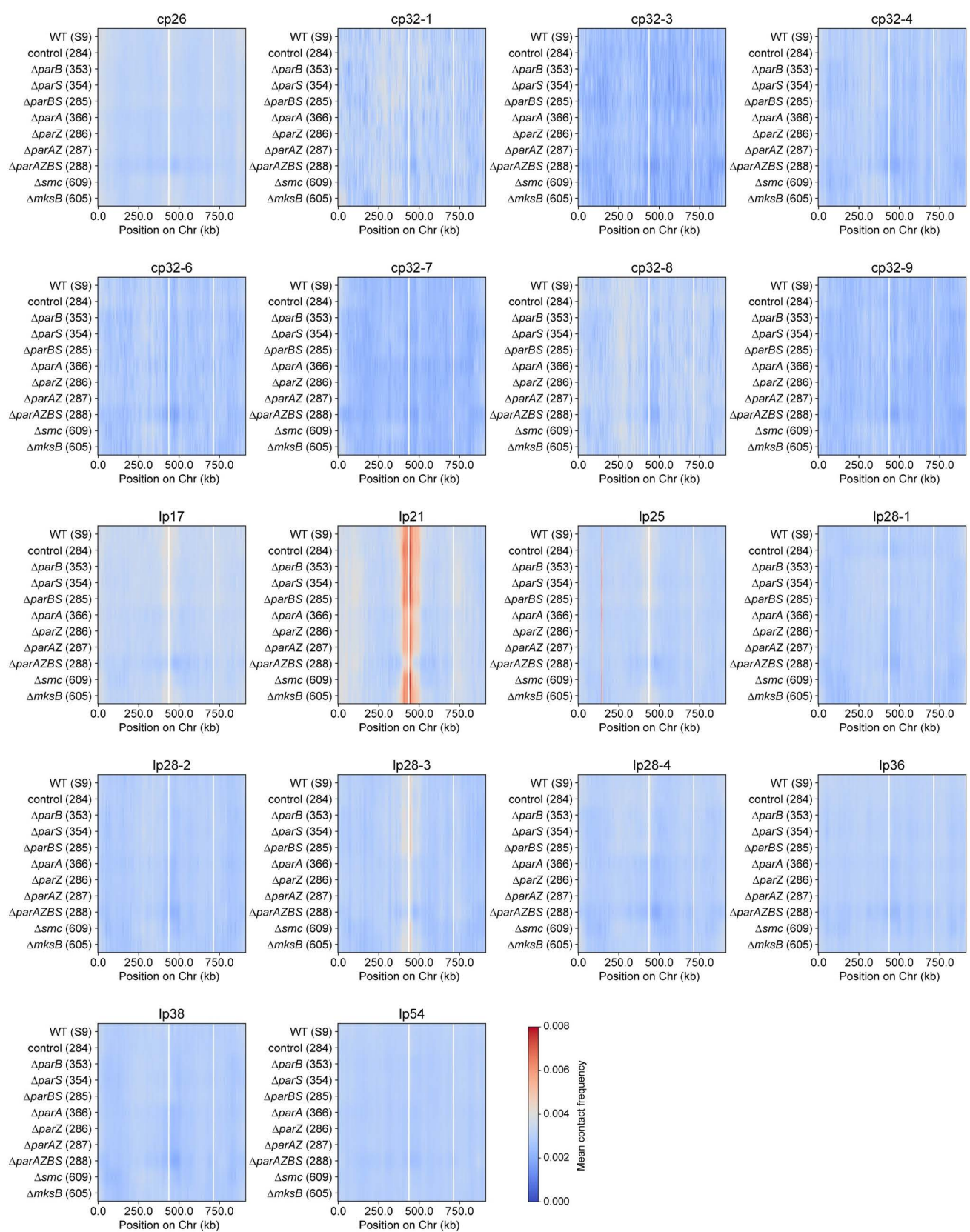
**S8 Fig. Plasmid-chromosome interactions in different mutants.**

Calculated plasmid-chromosome interaction frequencies are shown. The x-axis shows chromosome location in kb. The y-axis specifies the different plasmids analyzed. The color indicates the contact frequency between each plasmid and chromosome locus. Each graph plots the mean value of the two biological replicates shown in **S3 Fig**. Data are binned at 5-kb resolution. The data were normalized including all the interactions in the genome (i.e. intra-chromosomal, plasmid-chromosome and plasmid-plasmid interactions).



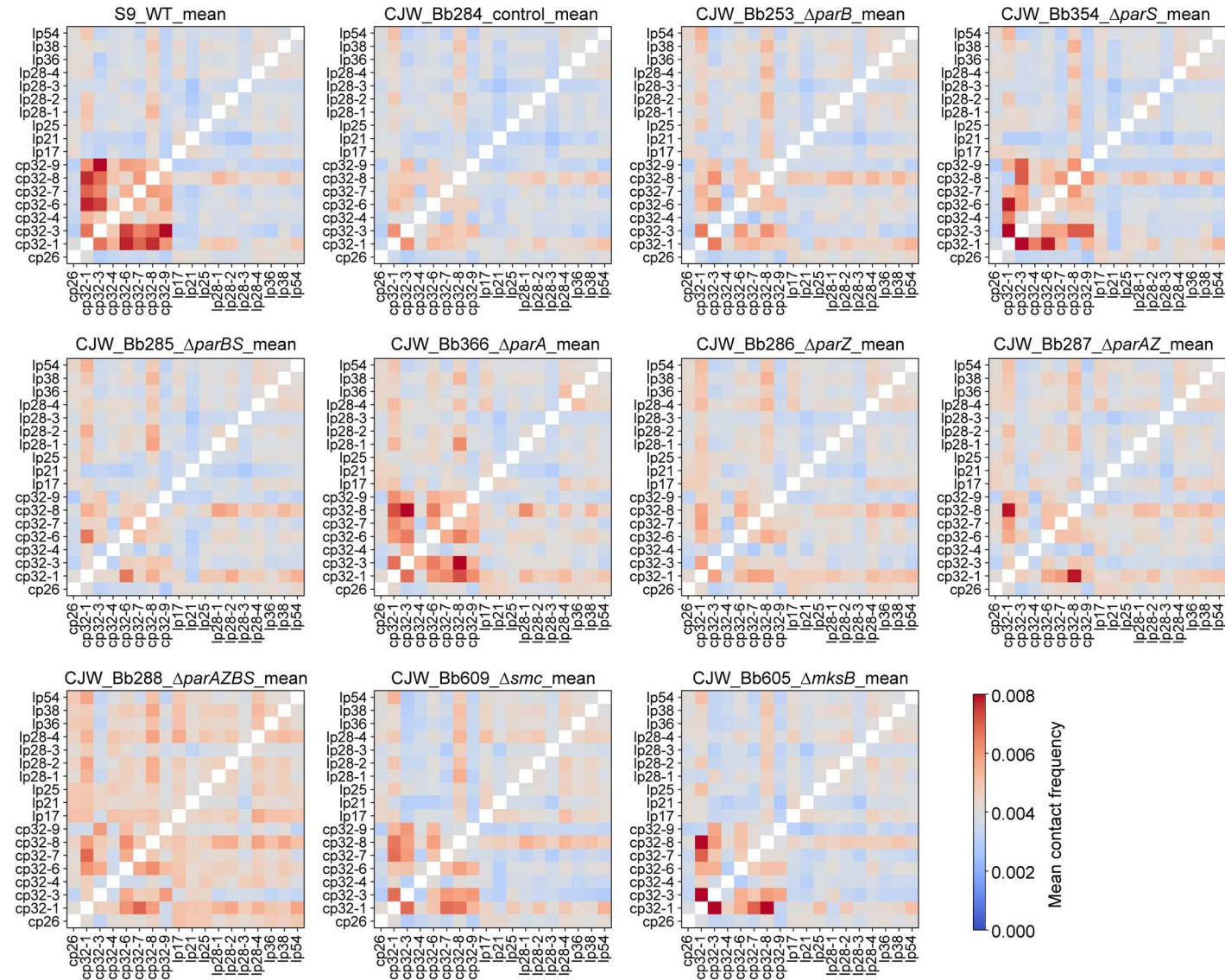
**S9 Fig. Renormalized plasmid-chromosome interactions in different mutants.**

Plasmid-chromosome interactions from **S8 Fig** were renormalized using iterative correction to remove the influence of intra-chromosomal and plasmid-plasmid interactions (see Materials and methods). The data were normalized such that each row had the same total score, and each column had the same total score.



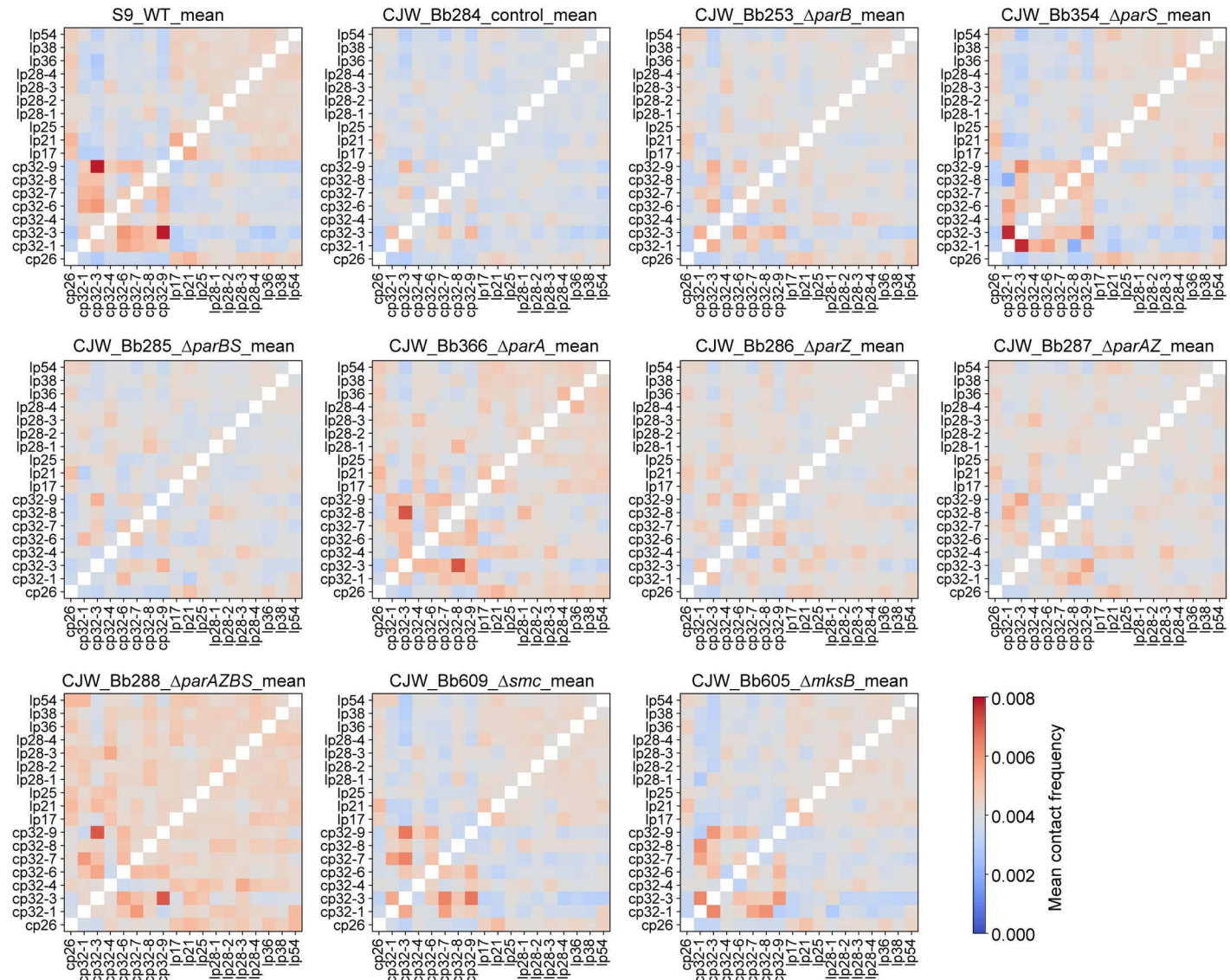
**S10 Fig. Plasmid-chromosome interactions in different mutants organized by plasmids.**

Calculated plasmid-chromosome interaction frequencies are shown. The x-axis shows the chromosome location in kb. The y-axis specifies the different mutants. The color indicates the contact frequency between each plasmid and chromosome locus. Each graph plots the mean value of the two biological replicates shown in **S3 Fig**. Data are binned at 5-kb resolution.



**S11 Fig. Plasmid-plasmid interactions in different mutants.**

Calculated plasmid-plasmid contact frequencies in different strains. The x- and y-axes indicate the plasmids analyzed. The color shows the computed contact frequency. Each graph plots the mean of the two biological replicates shown in **S3 Fig**. The data were normalized including all the interactions in the genome (i.e. intra-chromosomal, plasmid-chromosome and plasmid-plasmid interactions).



**S12 Fig. Renormalized plasmid-plasmid interactions in different mutants.**

Plasmid-plasmid contact frequencies from **S11 Fig** were renormalized without plasmid-chromosome interactions. The data were normalized such that each row had the same total score, and each column had the same total score.

**S1 Table. Bacterial strains used in this study.**

Strain	Genotype	Antibiotic resistance	Reference	Figure
S9	Transformable derivative of the <i>B. burgdorferi</i> type strain B31; lacks endogenous plasmids cp9, lp5, and lp56; also known as B31-A3-68- $\Delta bbe02::PflaB-aadA$	Sr	[1]	1-4, 5A-C, S1-S12
CJW_Bb284	S9-derived control strain; has gentamicin resistance cassette inserted between <i>parZ</i> and <i>parB</i>	Sr, Gm	[2]	5A-C, 6A, 6D-I, S3-S12
CJW_Bb285	S9-derived $\Delta parBS$ strain	Sr, Gm	[2]	5ABF, 7CF, S3-6, S8-12
CJW_Bb286	S9-derived $\Delta parZ$ strain	Sr, Gm	[2]	5ABG, 7HL, S3-6, S8-12
CJW_Bb287	S9-derived $\Delta parAZ$ strain	Sr, Gm	[2]	5ABG, 7IM, S3-6, S8-12
CJW_Bb288	S9-derived $\Delta parAZBS$ strain	Sr, Gm	[2]	5ABH, 7JN, S3-6, S8-12
CJW_Bb353	S9-derived $\Delta parB$ strain	Sr, Gm	[2]	5ABF, 7AD, S3-6, S8-12
CJW_Bb354	S9-derived $\Delta parS$ strain	Sr, Gm	[2]	5ABF, 7BE, S3-6, S8-12
CJW_Bb366	S9-derived $\Delta parA$ strain	Sr, Km	[2]	5ABG, 7GK, S3-6, S8-12
CJW_Bb605	S9-derived $\Delta mksB$ strain	Sr, Gm	This study	5ABE, 6CFI, S3-6, S8-12
CJW_Bb609	S9-derived $\Delta smc$ strain	Sr, Gm	[2]	5ABD, 6BEH, S3-6, S8-12

Sr, streptomycin resistance; Gm, gentamicin resistance; Km, kanamycin resistance.

## References

1. Rego RO, Bestor A, Rosa PA. Defining the plasmid-borne restriction-modification systems of the Lyme disease spirochete *Borrelia burgdorferi*. J Bacteriol. 2011;193(5):1161-71. Epub 2011/01/05. doi: 10.1128/JB.01176-10. PubMed PMID: 21193609; PubMed Central PMCID: PMC3067601.
2. Takacs CN, Wachter J, Xiang Y, Ren Z, Karaboja X, Scott M, et al. Polyploidy, regular patterning of genome copies, and unusual control of DNA partitioning in the Lyme disease spirochete. Nat Commun. 2022;13(1):7173. Epub 2022/12/01. doi: 10.1038/s41467-022-34876-4. PubMed PMID: 36450725; PubMed Central PMCID: PMC9712426.

**S2 Table. Plasmids used in this study.**

Plasmid	Description	Reference
<i>pΔmksB(gent)</i>	Plasmid to make replace <i>ΔmksB</i> with gentamycin resistance gene	This study
<i>pKIGent_parS<sup>P1</sup>_phoU</i>	Plasmid to insert <i>parS<sup>P1</sup></i> near <i>phoU</i>	[1]
<i>pΔparA(kan)</i>	Plasmid to delete <i>parA</i> from <i>B. burgdorferi</i> chromosome	[1]

**Reference**

1. Takacs CN, Wachter J, Xiang Y, Ren Z, Karaboga X, Scott M, et al. Polyploidy, regular patterning of genome copies, and unusual control of DNA partitioning in the Lyme disease spirochete. *Nat Commun.* 2022;13(1):7173. Epub 2022/12/01. doi: 10.1038/s41467-022-34876-4. PubMed PMID: 36450725; PubMed Central PMCID: PMCPMC9712426.

**S3 Table. Oligonucleotides used in this study.**

Oligo	Sequence
NT968	5'-tggtaccgagctcgatccggattttgcgttgttagactactacatgtcc-3'
NT969	5'-tttggtttttacccggcccgattgtctaaaagaagtatcgaaattcaactcatg-3'
NT970	5'-cttcatttaagacaatcggggccgggtaaaaaaaaacaaaagatccttaaaggatctttg-3'
NT971	5'-tatgccaatttgcgcgcggtaaggaagattcctattaaggtaacttaagagc-3'
NT972	5'-aatcttccttgaaccgcggcgacaaaattggcataattccatgtttctatttgaagg-3'
NT973	5'-ctcttagatgcattgcataaccaaaaagatataaccgaaaagacaataatgc-3'
NT974	5'-tcattttgggtattgcaatgcattgcattgcattgcattgcattgcattgcattgc-3'
NT975	5'-aaacaacgcaaaagaatccggatccgagctcggtaccaagcttgcatacgcttgc-3'

**S4 Table. Next generation sequencing samples used in this study.**

Sample name	Figure	Reference	Identifier	Numbers of nonduplicated double-side unique mapped reads
HiC_CJW_Bb284_rep1	5A-C, 6A, 6D-I, S3-S12	This study	<a href="#">GSM7056005</a>	12,949,960
HiC_CJW_Bb284_rep2	5A-C, 6D-I, S3-S12	This study	<a href="#">GSM7056006</a>	18,388,642
HiC_CJW_Bb285_rep1	5ABF, 7CF, S3-6, S8-12	This study	<a href="#">GSM7056007</a>	15,384,363
HiC_CJW_Bb285_rep2	5ABF, S3-6, S8-12	This study	<a href="#">GSM7056008</a>	17,196,945
HiC_CJW_Bb286_rep1	5ABG, 7HL, S3-6, S8-12	This study	<a href="#">GSM7056009</a>	16,232,326
HiC_CJW_Bb286_rep2	5ABG, S3-6, S8-12	This study	<a href="#">GSM7056010</a>	18,775,364
HiC_CJW_Bb287_rep1	5ABG, 7IM, S3-6, S8-12	This study	<a href="#">GSM7056011</a>	14,421,014
HiC_CJW_Bb287_rep2	5ABG, S3-6, S8-12	This study	<a href="#">GSM7056012</a>	16,560,484
HiC_CJW_Bb288_rep1	5ABH, 7JN, S3-6, S8-12	This study	<a href="#">GSM7056013</a>	15,605,994
HiC_CJW_Bb288_rep2	5ABH, S3-6, S8-12	This study	<a href="#">GSM7056014</a>	17,741,544
HiC_CJW_Bb353_rep1	5ABF, 7AD, S3-6, S8-12	This study	<a href="#">GSM7056015</a>	15,306,050
HiC_CJW_Bb353_rep2	5ABF, S3-6, S8-12	This study	<a href="#">GSM7056016</a>	13,407,970
HiC_CJW_Bb354_rep1	5ABF, 7BE, S3-6, S8-12	This study	<a href="#">GSM7056017</a>	13,917,027
HiC_CJW_Bb354_rep2	5ABF, S3-6, S8-12	This study	<a href="#">GSM7056018</a>	11,211,083
HiC_CJW_Bb366_rep1	5ABG, 7GK, S3-6, S8-12	This study	<a href="#">GSM7056019</a>	15,375,430
HiC_CJW_Bb366_rep2	5ABG, S3-6, S8-12	This study	<a href="#">GSM7056020</a>	10,765,224
HiC_CJW_Bb605_rep1	5ABE, 6I, S3-6, S8-12	This study	<a href="#">GSM7056021</a>	8,440,508
HiC_CJW_Bb605_rep2	5ABE, 6CFI, S3-6, S8-12	This study	<a href="#">GSM7056022</a>	9,953,656
HiC_CJW_Bb609_rep1	5ABD, 6BEH, S3-6, S8-12	This study	<a href="#">GSM7056023</a>	9,798,914
HiC_CJW_Bb609_rep2	5ABD, 6H, S3-6, S8-12	This study	<a href="#">GSM7056024</a>	11,279,804
HiC_CJW_S9WT_rep1	1-4, 5A-C, S1-S12	This study	<a href="#">GSM7056025</a>	10,377,706
HiC_CJW_S9WT_rep2	5A-C, S1-S12	This study	<a href="#">GSM7056026</a>	11,847,047